

## Electric field-induced layer deformations in the subphases of an antiferroelectric liquid crystal device

L. S. Matkin, H. F. Gleeson,<sup>a)</sup> L. J. Baylis, S. J. Watson, and N. Bowring  
*Department of Physics and Astronomy, University of Manchester, Manchester M13 9PL, United Kingdom*

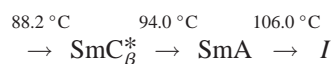
A. Seed, M. Hird, and J. W. Goodby  
*Department of Chemistry, Hull University, Hull HU6 7RJ, United Kingdom*

(Received 5 April 2000; accepted for publication 22 May 2000)

The layer structure in the antiferroelectric, ferrielectric, and ferroelectric phases of a liquid crystal device is reported, together with its electric field-induced deformation. The field-free chevron angle is comparable to the steric tilt angle, but differs significantly from the optical tilt angle. A sharp field threshold is observed for the chevron to bookshelf transition in the antiferroelectric phase at 1.3 V/ $\mu\text{m}$ , while layer deformations occur at much lower fields (0.3 V/ $\mu\text{m}$ ) in the other subphases. Models are proposed for the layer deformations. © 2000 American Institute of Physics. [S0003-6951(00)00129-7]

Ferroelectric liquid crystals are formed from rodlike chiral molecules, arranged in layers with their average molecular direction (director) tilted with respect to the layer normal by a temperature-dependent angle.<sup>1</sup> Within a device the director defines the optic axis and is readily switched to positions on either side of a symmetry axis by an electric field, providing an electro-optic switch. The tilt angle increases with decreasing temperature and the resulting change in layer spacing usually induces a chevron structure in a device,<sup>2</sup> which is transformed to a bookshelf geometry on application of a sufficiently high electric field<sup>3,4</sup> (Fig. 1). The complex director configurations that can be accommodated by the chevron structure influence device electro-optic properties, so it is important to study both the chevron structure and its field-induced changes in liquid crystal devices. This can be done effectively by x-ray diffraction. Such studies are also relevant to antiferroelectric and ferrielectric liquid crystals, though there are few reports of the temperature dependence<sup>5</sup> or field response<sup>6,7</sup> of the chevron structure in the antiferroelectric phase, and none in ferrielectric phases. This paper presents the temperature dependence of the chevron structure in a material exhibiting ferro-, ferri-, and antiferroelectric phases, together with the evolution of the field-induced layer deformations in each of the chiral subphases. The measurements are discussed in context with electro-optic studies of the same device.

The material used, denoted AS573, was synthesized at Hull University, UK and has been studied extensively.<sup>8-10</sup> The phase sequence determined electro-optically is



(notation is as used elsewhere<sup>8-10</sup>). The switching behavior

in the ferroelectric phase is unusual so this phase has been denoted the  $\text{SmC}_\beta^*$  phase to distinguish it from conventional ferroelectric liquid crystals.

X-ray scattering studies were carried out on a liquid crystal device at Daresbury SRS, UK, as described previously.<sup>11,12</sup> The liquid crystal device was constructed from two 300- $\mu\text{m}$ -thick indium-tin-oxide coated glass plates assembled to enclose a liquid crystal sample approximately 15  $\mu\text{m}$  in thickness. The sample was aligned in a planar geometry using a rubbed nylon alignment layer and held in a temperature controlled environment. Rocking curves were produced by integrating the intensity of the Bragg scattering peak from the device at specific angles,  $\theta$ , to the  $0^\circ$  position as defined by the geometry in Fig. 2. Data were normalized to take account of the angular dependence of the glass absorption and the chevron angle was found to within  $\pm 0.5^\circ$  from the curves. Rocking curves provide information on the range of layer tilts in the sample; a bookshelf structure produces an intense peak when  $\theta \sim 0^\circ$ , whereas a chevron structure gives intense peaks when the device is held at the chevron angle ( $\theta = \pm \delta$ ).

The chevron angle,  $\delta$ , in the device increases rapidly at the  $\text{SmA}$  to  $\text{SmC}_\beta^*$  transition, reaching a plateau approximately  $10^\circ\text{C}$  below the transition (Fig. 3). The chevron angle compares well with the tilt angle of the material deduced from powder diffraction methods (steric tilt), but is significantly different from that measured by electro-optic means.<sup>13</sup> The crossover of the optical and steric tilt implies changes in molecular configuration as a function of temperature.<sup>9,13</sup> Since the chevron angle is related to the steric rather than optical tilt angle, it is significantly lower

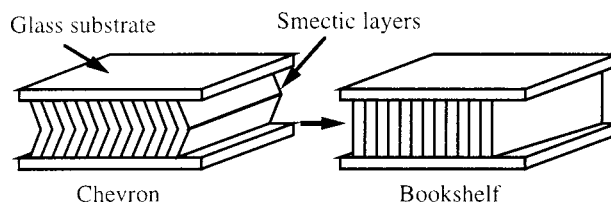


FIG. 1. The chevron and bookshelf device geometries.

<sup>a)</sup>Author to whom all correspondence should be addressed; electronic mail: Helen.Gleeson@man.ac.uk

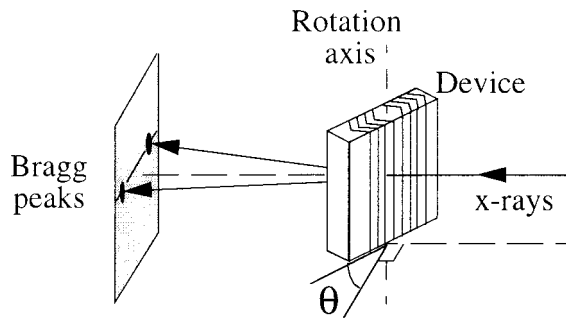


FIG. 2. The geometry of the experiment.

than that measured in many ferroelectric devices.<sup>1</sup>

The evolution of the field-induced chevron to bookshelf transition was investigated in several of the chiral subphases of AS573. At each chosen temperature the device was held at a fixed angle,  $\theta$ , to the incident x-ray beam and a 150 Hz ac voltage applied. The voltage was increased gradually and each incremental voltage was held for approximately 1 min while the x-ray scattering intensity was measured, making the experiment essentially static. The procedure was repeated at several angles for each temperature, the data providing information about the voltage dependence of layers tilted at particular angles to the device substrates. Prior to each electric-field deformation experiment, the device was heated to the untilted smectic-A phase then cooled slowly to the selected temperature to produce identical initial field-off structures. The graphs in Fig. 4 show details of the field-induced layer deformations observed in specific chiral subphases. The cartoons in the figure show schematics of field-induced layer deformations deduced from the x-ray data collected at each angle. The electric field-induced response of the layers varies significantly from phase to phase.

The chevron to bookshelf transition in the antiferroelectric phase is shown in Fig. 4(a). At 0 V, a large intensity is measured with the device held at  $\theta = \delta$  from layers in the chevron structure. A much smaller contribution comes from layers in the bookshelf geometry (device at  $0^\circ$ ). The chevron to bookshelf transition has a distinct threshold at around 1.3 V/ $\mu\text{m}$  (20 V for the device studied). Above this threshold, the scattering intensity obtained with the device at  $\theta = \delta$  falls

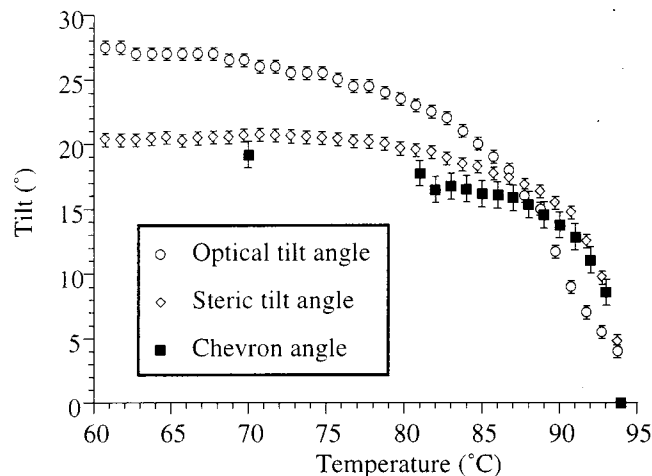


FIG. 3. The temperature dependence of the device chevron angle compared with the steric and optical tilt angle measurements.

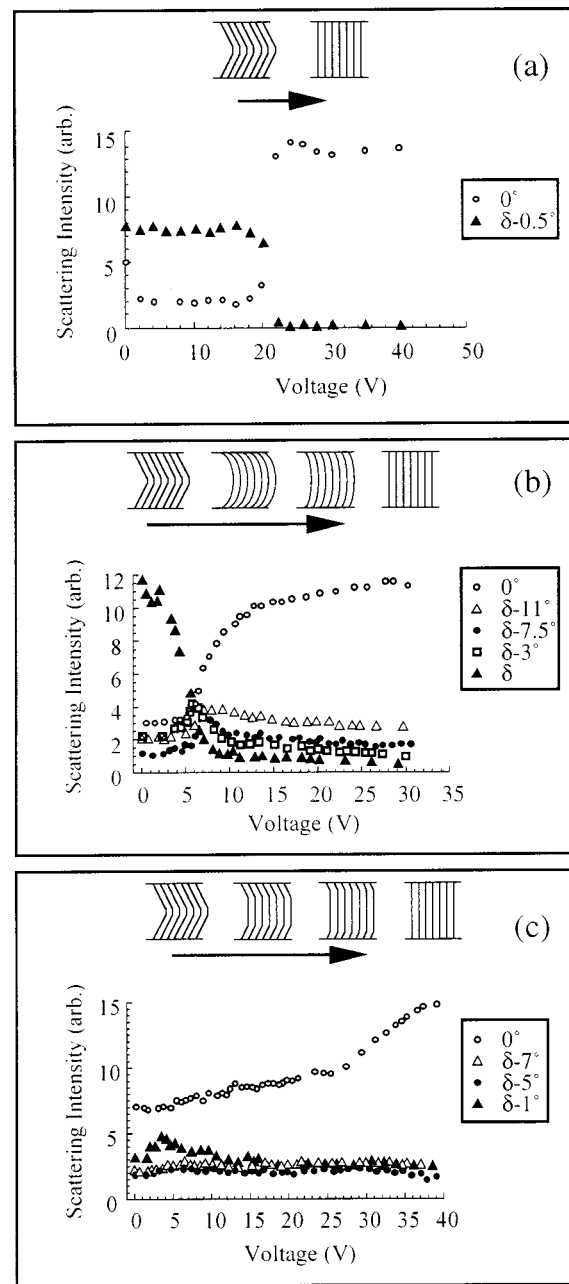


FIG. 4. X-ray scattering intensity as a function of applied voltage for different angles  $\theta$  (defined in Fig. 2) in (a) the antiferroelectric phase (70 °C), (b) the AFE phase (85 °C), and (c) the  $\text{SmC}_\beta^*$  phase (92 °C).

to zero, while the contribution from a bookshelf structure increases.

The field-induced layer deformations in the ferroelectric and high temperature AFE phases are quite different from that in the low temperature antiferroelectric phase, Fig. 4(b). The layer reorientation begins at around 5 V (0.3 V/ $\mu\text{m}$ ), a much lower field than in the antiferroelectric phase. The data suggest a curved intermediate structure [cartoon in Fig. 4(b)], rather than the sharp transition seen in the antiferroelectric phase; on application of 6 V (0.4 V/ $\mu\text{m}$ ) there are similar scattering contributions from layers measured at angles between  $0^\circ$  and the chevron angle.

At the temperature chosen for study in the  $\text{SmC}_\beta^*$  phase, the chevron angle was  $12^\circ$  and the layer structure also included a significant amount of bookshelf geometry [see the cartoon in Fig. 4(c)]. The scattering intensity data from the

device held at  $0^\circ$  indicate that increasing the applied voltage gradually increases the proportion of layers in the bookshelf geometry. No distinct threshold was observed. There was no significant scattering observed at intermediate angles, though the layers appear to move through angles slightly smaller than the chevron angle at low voltages. A possible structural evolution for this phase is shown in Fig. 4(c). There may be a small change in the chevron angle of the remaining layers. The thresholdless behavior is consistent with optical transmission measurements of this device, but is unusual for ferroelectric liquid crystals.

All the thresholds for layer motion are low compared to those observed in ferroelectric devices<sup>1</sup> (around 6–15 V/ $\mu\text{m}$ ), though the antiferroelectric chevron to bookshelf threshold is comparable to that reported for a different material<sup>6</sup> (3.5 V/ $\mu\text{m}$ ). The different field induced layer deformations in the subphases cannot be attributed to the electric torque as there is negligible variation in spontaneous polarization over the temperature range studied. The threshold differences must therefore be due to variations in layer elastic constants or in molecular arrangement between phases.

This work was funded by the Engineering and Physical Sciences Research Council. Two of the authors (L.B. and

L.M.) gratefully acknowledge funding from the Defense Evaluation Research Agency and Lucent Technologies.

- <sup>1</sup>J. W. Goodby *et al.*, *Ferroelectric Liquid Crystals, Principles, Properties and Applications* (Gordon and Breach, Philadelphia, PA, 1991).
- <sup>2</sup>T. P. Reiker, N. A. Clark, G. S. Smith, D. S. Parmar, E. B. Sirota, and C. R. Safinya, *Phys. Rev. Lett.* **59**, 2658 (1987).
- <sup>3</sup>J. S. Patel, S.-D. Lee, and J. W. Goodby, *Phys. Rev. A* **40**, 2854 (1989).
- <sup>4</sup>G. Srajer, R. Pindak, and J. S. Patel, *Phys. Rev. A* **43**, 5744 (1990).
- <sup>5</sup>P. Cluzeau, P. Barois, H. T. Nguyen, and C. Destrade, *Eur. Phys. J. A* **3**, 73 (1998).
- <sup>6</sup>M. Johno, A. D. L. Chandani, Y. Ouchi, H. Takezoe, A. Fukuda, M. Ichihashi, and K. Furukawa, *Jpn. J. Appl. Phys., Part 2* **28**, L119 (1989); M. Johno, Y. Ouchi, H. Takezoe, A. Fukuda, K. Trashima, and K. Furukawa, *ibid.* **29**, L111 (1990).
- <sup>7</sup>K. Itoh, M. Johno, Y. Ouchi, H. Takezoe, and A. Fukuda, *Jpn. J. Appl. Phys., Part 1* **30**, 735 (1991).
- <sup>8</sup>Y. Panarin, O. Kalinovskaya, and J. K. Vij, *Phys. Rev. E* **55**, 4345 (1997).
- <sup>9</sup>H. F. Gleeson *et al.*, *Liq. Cryst.* **26**, 1415 (1999).
- <sup>10</sup>L. J. Baylis, H. F. Gleeson, A. J. Seed, P. J. Styring, M. Hird, and J. W. Goodby, *Mol. Cryst. Liq. Cryst. Sci. Technol., Sect. A* **328**, 13 (1999).
- <sup>11</sup>A. S. Morse and H. F. Gleeson, *Liq. Cryst.* **23**, 531 (1997).
- <sup>12</sup>H. F. Gleeson, C. Carboni, and A. S. Morse, *Rev. Sci. Instrum.* **66**, 3563 (1995).
- <sup>13</sup>J. T. Mills, H. F. Gleeson, M. Hird, P. Styring, and J. W. Goodby, *J. Mater. Chem.* **8**, 2385 (1998).